Tow-Steered Panels with Holes Subjected to Compression or Shear Loading

Dawn C. Jegley*
NASA Langley Research Center, Hampton, Virginia 23681

Brian F. Tatting†
ADOPTECH, Inc., Blacksburg, Virginia 24060

and

Zafer Gürdal‡
Virginia Tech, Blacksburg, Virginia, 24061
Delft University of Technology, 2629 HS Delft, The Netherlands

Tailoring composite laminates to vary the fiber orientations within a fiber layer of a laminate to address non-uniform stress states and provide structural advantages such as the alteration of principal load paths has potential application to future low-cost, light-weight structures for commercial transport aircraft. Evaluation of this approach requires the determination of the effectiveness of stiffness tailoring through the use of curvilinear fiber paths in flat panels including the reduction of stress concentrations around the holes and the increase in load carrying capability. Panels were designed through the use of an optimization code using a genetic algorithm and fabricated using a tow-steering approach. Manufacturing limitations, such as the radius of curvature of tows the machine could support, avoidance of wrinkling of fibers and minimization of gaps between fibers were considered in the design process. Variable stiffness tow-steered panels constructed with curvilinear fiber paths were fabricated so that the design methodology could be verified through experimentation. Finite element analysis where each element's stacking sequence was accurately defined is used to verify the behavior predicted based on the design code. Experiments on variable stiffness flat panels with central circular holes were conducted with the panels loaded in axial compression or shear. Tape and tow-steered panels are used to demonstrate the buckling, post-buckling and failure behavior of elastically tailored panels. The experimental results presented establish the buckling performance improvements attainable by elastic tailoring of composite laminates.

* Senior Aerospace Engineer, Mechanics of Structures and Materials Branch, MS 190, Associate Fellow, AIAA
† Research Scientist, 2000 Kraft Drive, Suite 1204, Blacksburg, VA 24060.
‡ Professor, Departments of Engineering Science and Mechanics, and Aerospace and Ocean Engineering, Virginia Tech, Blacksburg, VA 24061; currently Chair, Faculty of Aerospace Structures, Delft Technical University, Kluyverweg 1, 2629 HS Delft, The Netherlands, Associate Fellow, AIAA.

I. Introduction

One of NASA's goals is to reduce the weight of a subsonic aircraft by 20% in the next 15 years. To achieve this goal, NASA has been involved in the development of technologies needed for future low-cost, light-weight composite structures for commercial transport aircraft. One such technology involves the elastic tailoring of structures. Elastic tailoring implies that the stiffness characteristics within a structure can be manipulated by the designer to utilize the material with respect to strength and stability constraints. As a simple example, the directionality of composite materials that possess high stiffness-to-weight and strength-to-weight ratios has long been utilized to improve the performance of a multi-layered laminate under an expected load state, principally through stacking sequence optimization.[1]

Modern extensions to the stacking sequence design methodology include the possibility for the fiber orientation angle to vary within each layer, producing laminates with spatially-varying stiffness characteristics.[2-4] This variation implies that the fibers must follow non-geodesic paths, which translates to curvilinear (non-straight) paths for flat laminate geometries. Research in this area in the early 1990's demonstrated the effectiveness of this technique to improve the buckling response of flat rectangular laminates subjected to in-plane loading, however these results are primarily analytical/numerical in nature.[5,6] Initial presentation of the theoretical findings invariably prompted questions regarding the manufacturability of the curvilinear fiber paths and the necessity for experimental verification. Toward this end, the parameters controlling the variation of the fiber orientation angle were refined to correspond with an emerging manufacturing technique for fabricating fiber-reinforced layers using non-geodesic paths.[7] The manufacturing technique is commonly referred to as tow-placement, and consists of laying down multiple tows of composite material tape along a pre-defined path using computer-controlled machinery. By feeding out individual tows at different rates, curved paths could be constructed subject to various manufacturing limits.[8] Subsequent research involved building prototypes of these "tow-steered" panels to verify manufacturability issues along with mechanical testing to prove that the performance improvements promised by the analytical estimations existed.[9-11] The fabrication issues associated with tow-placement of the curvilinear fiber paths is the topic of another paper within this forum,[12] while this paper addresses the ensuing mechanical testing and response verification.

The tow-steering design techniques studied herein are applied to flat panels with a central hole subjected to in-plane loading. This problem has often been studied in association with elastic tailoring due to the disparity of the stress states between the far field and local regions around the hole. Earlier work demonstrates excellent correlation between predicted buckling loads and experimental results for panels subjected to compressive loading.[13] Subsequent design studies prompted additional investigations concerning arbitrary hole placement and shear loading of tow-steered panels.[14] Experimental results and comparisons to finite-element predictions are presented for panels subjected to compression or shear loading. Finally, conclusions are drawn from the trends revealed from these studies. These trends point a way toward further application of the tow-steering design concepts for realistic aeronautical structures.

II. Panel Design

The prototype tow-steered designs that were manufactured and tested are based on a design study conducted in 2002 for a flat rectangular panel with a central hole subjected to compressive loading.[15] The design procedure is fully described in reference 15, so a detailed discussion is not included here. In summary, analytical and finite-element analyses were used in conjunction with specialized laminate design software to generate tow-steered designs that exhibited increased buckling loads compared to traditional straight-fiber laminates of similar weight. The best configurations generally consisted of stiff/thick regions at the edges of the panels with a softer/thinner center area. This arrangement effectively unloaded the material around the central hole and drove the load toward the stiffer and/or thicker regions. Correlation between the finite-element predictions and the experimental results for the first set of these prototype designs was reported in reference 13, with excellent agreement between the predicted and experimental behavior.

A subsequent study integrated the analysis capabilities of a shell finite-element analysis code (STructural Analysis of General Shells - STAGS 4[16]) within the design environment to achieve an automated process that can handle more complex geometries and loading.[14] This new tool was used to verify the results from the original design study (which was based on simpler methods of analysis that neglected the central hole) and to investigate in-plane shear loading. In addition to confirming that the prototype designs were excellent candidates for increasing the compressive buckling load, a new mechanism was discovered for laminates using the overlap ply construction method that also showed potential for many structural applications. This ply construction technique allows neighboring tows of material to overlap at their edges, which produces thickness variation for curvilinear fiber paths. Previously, this thickness increase was situated near the edges of the panels to unload the center region that

contained the hole. However, it was found that for shear loading and for smaller sizes of the central hole under compression, a built-up region in the center of the panel also provided an increase in the buckling load. In these cases, the increase in bending stiffness provided by the thicker laminate offset the elevated stresses that resulted from the stiffer central region.

The presence of this new possibility for elastic tailoring prompted renewed interest in experimental verification of the tow-steering design concepts. Fortunately, a second set of manufactured specimens was available using the original layups designed for compression. Though the laminates did not exactly correspond to those that followed the new mechanism discovered in the latest design study, the similar stiffening aspect of the overlap technique provided an opportunity to investigate the effect of a hole within the stiffer region of a tow-steered laminate. It was surmised that if a panel could adequately withstand a hole introduced into the stiffer region of the laminate, while already proving that a hole in the softer region did not drastically inhibit the buckling load, an improvement in overall damage tolerance could be justified. Shear loading was also performed using the original prototype layups, though it should be noted that the prototype designs were intended for compression loading and are investigated for shear loading due to their availability and to validate agreement between numerical and actual response.

III. Test Panels

The optimized curvilinear fiber paths were translated into a computer-controlled tow placement machine using Cincinnati Machine's ACRAPLACE software. Two large sheets each of traditional unidirectional plies, a tow-drop design, and an overlap design were fabricated by Cincinnati Machine. One sheet of each construction was divided into four rectangular panels which were 24 inches long and 15 inches wide. Central circular holes with a diameter of 1.5 or 3.0 inches were machined into the panels. These panels are described in reference 13 and are shown in Figure 1 as indicated by the gray lines. The overlap construction method is shown in the figure to indicate the thicker/stiffer

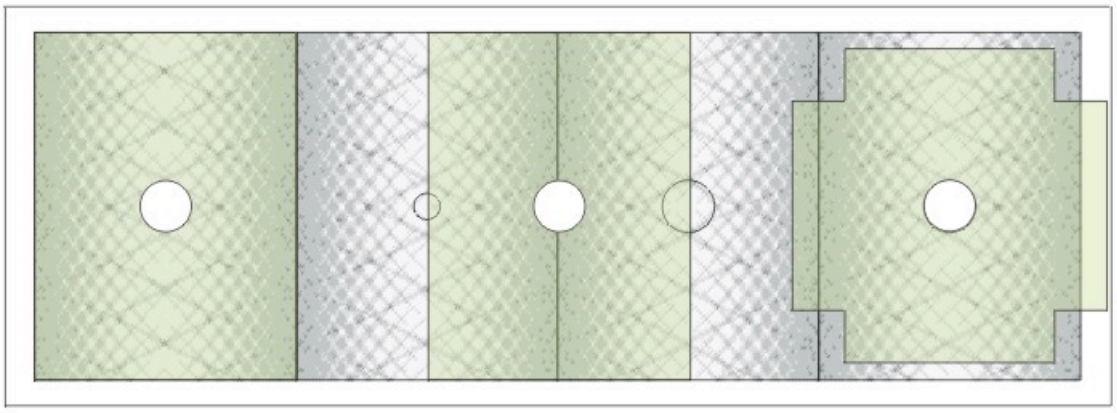

Figure 1. Specimen geometry from manufactured laminate sheet.

regions of the specimens, where the gray shaded regions represent the thickness of the laminate due to the overlaps. The second sheet of each construction method was cut into new panel geometries: one rectangular panel with a 3-inch diameter central hole was repeated for a comparison to previous work; an offset panel with the same dimensions as the previous panels but with the central hole located in the stiffer region; and a square shear specimen with a central circular hole, initially 17.5 inches on each side. This cut pattern is indicated in Figure 1 by the green shaded regions.

The configuration for the compression-loaded panels is shown in Figure 2. The top and bottom edges of the compression specimens each extend two inches into the potting material producing a 20-inch gage length. These ends are then ground flat and parallel. The unloaded edges of the specimen are constrained by knife-edge supports that are approximately one-third of an inch from the longitudinal edges of the panel. The knife-edge supports constrain the out-of-plane displacement and rotation about the horizontal axis. A panel with a 3-inch diameter hole loaded into the testing fixture is shown in Figure 2b.

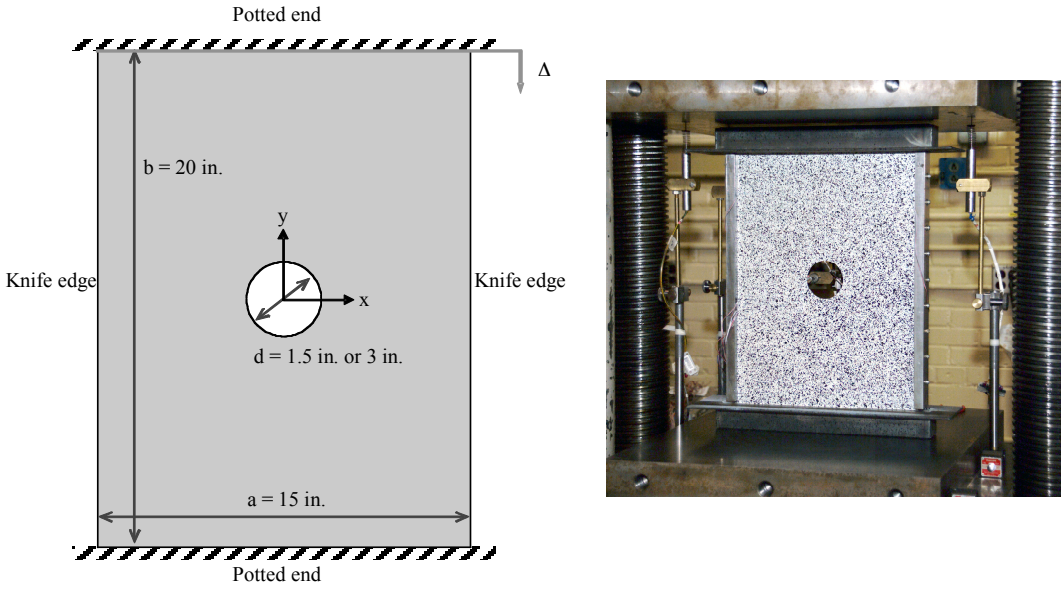

a) Panel Geometry b) Testing fixture

Figure 2. Geometry and testing configuration for axial compression.

The configuration for the shear-loaded panels is shown in Figure 3. The shear panels require flat and parallel surfaces for connection to the test fixture so metal doublers were bonded to the exterior 2.75 inches on each surface and then the assembly ground flat and parallel. Additionally, the corners outside the doublers were removed as shown in Figure 3. The doubler regions were drilled to match a picture-frame fixture that uses a mechanical test technique as described in reference 17. A shear panel loaded in the picture-frame fixture is shown in Figure 3b.

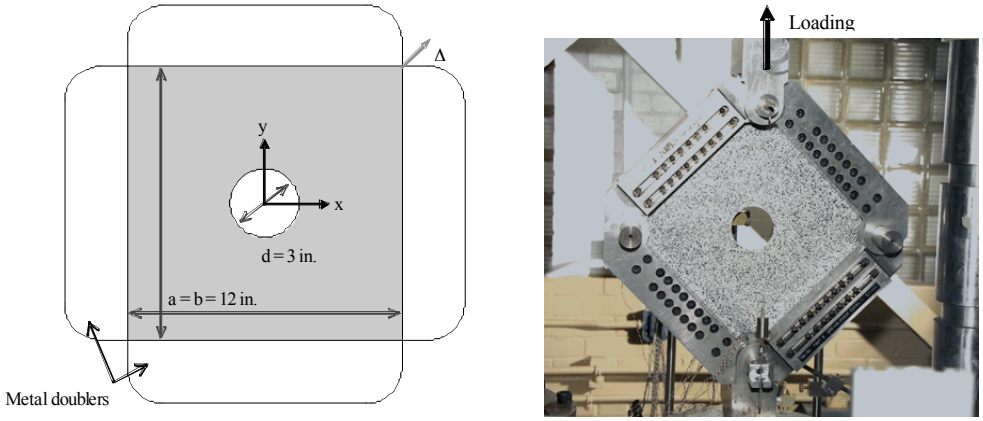

a) Panel Geometry b) Testing fixture

Figure 3. Geometry and testing configuration for in-plane shear.

Each panel was instrumented with strain gages and Direct Current Displacement Transducers (DCDTs). Back-to-back strain gages were located as shown in Figure 4a and Figure 5a for compression- and shear-loaded panels, respectively. Two DCDTs were used to measure end-shortening and two were used to measure out-of-plane displacement for each specimen. An out-of-plane displacement measurement was taken at the axial quarter point directly above the center of the specimen and another was taken close to the hole, at the mid-length location. DCDT locations are shown in Figure 4b and Figure 5b for the compression-loaded and shear-loaded panels, respectively.

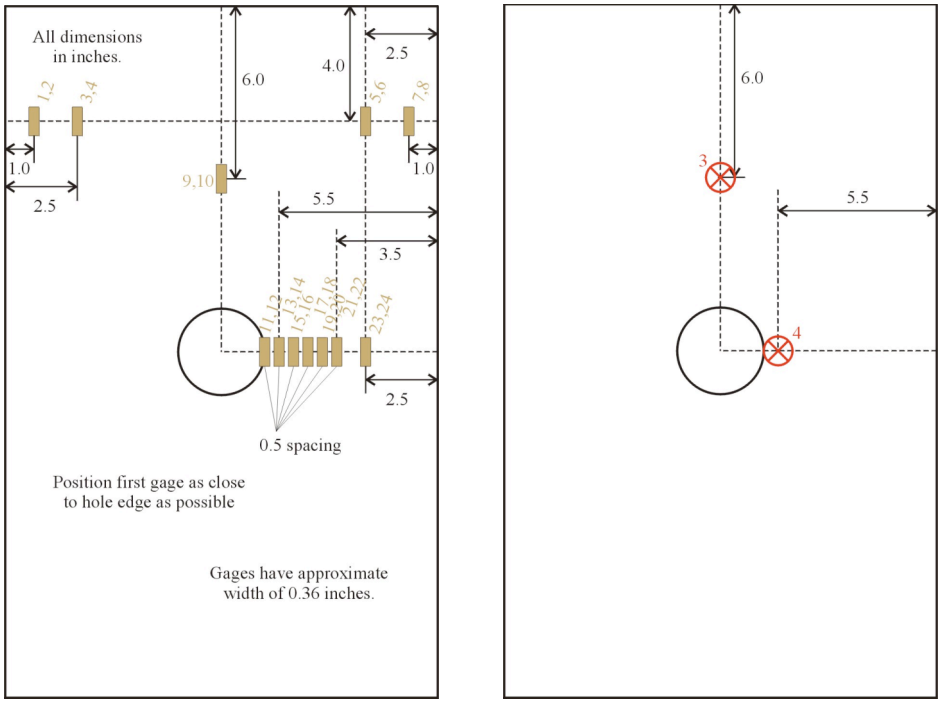

a) Strain gage locations b) DCDT locations

Figure 4. Strain gage and DCDT locations for compression specimens

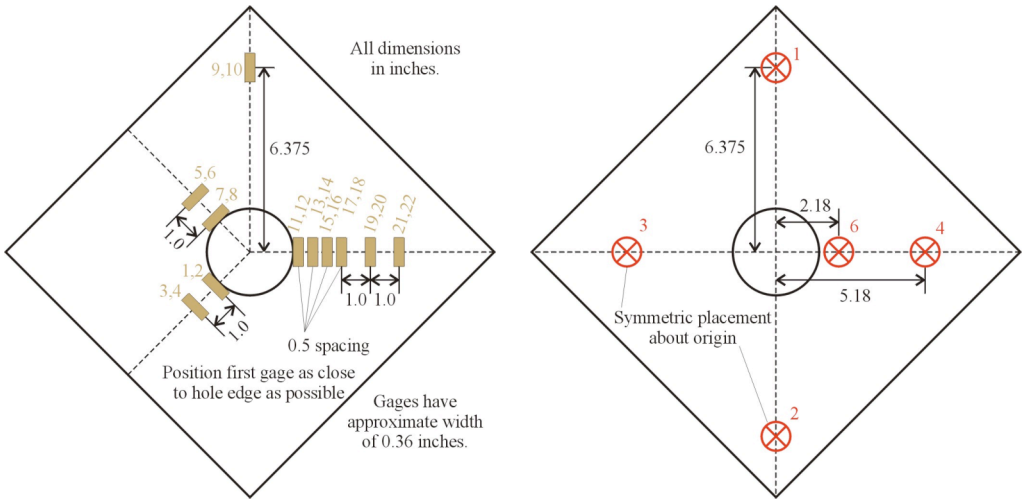

a) Strain gage locations b) DCDT locations

Figure 5. Strain gage and DCDT locations for shear specimens.

A summary of the test specimen geometries is presented in Table 1. Panels are identified by construction techniques: A, straight-fiber; B, tow-drop; and C, overlap. Specimens 1-4 of each construction technique were painted white prior to testing and a shadow Moiré interferometry technique was used to monitor out-of-plane displacement patterns to qualitatively identify buckle patterns and changes in out-of-plane deformation during loading. Specimens 5-7 of each series were painted with a "speckle pattern" so that a 3D optical system could be used to monitor the deformations and calculate strains for each specimen. This speckle pattern is observable in the photographs of Figure 2 and Figure 3. The optical systems uses two cameras and a computer to record the deformation pattern of the panel surface at regular intervals, in this case, once every 10 seconds. The computer calculates the motion of each location based on the two photographs from different angles to the surface of the specimen. In-plane displacements and strains and out-of-plane displacements can accurately be determined based on

Table 1: Panel identification

Geometry		No hole	1.5-in. hole	3.0-in. hole in un-stiffened region	3.0-in. hole in stiffened region	No hole	3.0-in. hole
Loading		Compression				Shear	
Construction Technique	Straight-fiber	A1	A2	A3, A4, **A5**		A8	**A7**
	Tow-drop		B1, B2	B3, B4, **B5**	**B6**		**B7**
	Overlap		C1, C2	C3, C4, **C5**	**C6**		**C7**

these photographs. A full description of this technique is presented in reference 18. Each specimen was loaded to failure at a rate of approximately 1,000 lb/min.

IV. Results and Discussion

Analytical predictions for structural response, including deformation and nonlinear behavior, is based on the shell finite element code STAGS.[16] Models for both compression and shear were constructed using an average size element of one-quarter inch edge length, and the potted and doubler regions are also modeled to provide better correlation with the mechanical testing conditions. The meshes used for compression- and shear-loaded panels are shown in Figure 6 and, respectively, where the darker regions represent the potted and doubler regions. Stiffness variation of tow-steered panels is calculated through an automated procedure implemented via a user-defined subroutine in STAGS, as explained in reference 14.

The following process is used to generate the nonlinear solution using STAGS. First, a linear bifurcation analysis is performed and the first two buckling modes are calculated. Second, the finite element model is re-defined with the buckling modes introduced as small initial imperfections with magnitude of 0.001 inches. The inward/outward directions of the imperfections are determined through trial-and-error until the nonlinear response matches the behavior of the out-of-plane displacement as observed during the test. Third, a nonlinear solution is determined for loads up to the load level attained in the test. Re-starts are often used to ensure that the mode switching phenomenon is captured and that the analytical deformation corresponds to the actual response of the specimen. In-plane and out-of-plane displacements for the DCDT locations are output to compare with the experimental results.

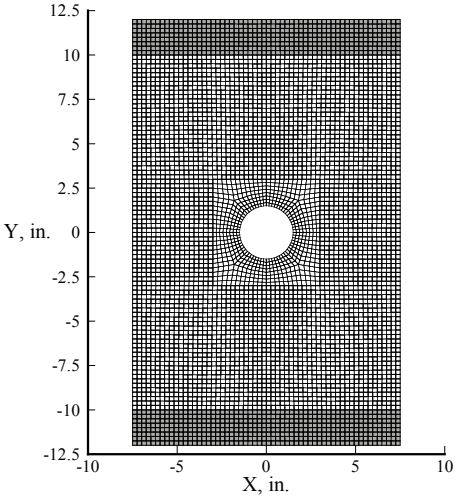

Figure 6. STAGS mesh for compression loading.

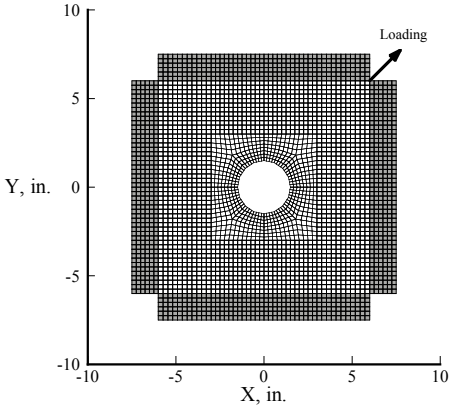

Figure 7. STAGS Mesh for shear loading.

A. Compression Loaded Panels

Eleven panels were subjected to compressive loading in the previous study[13] and five additional panels were subjected to compressive loading in the current study. Each panel had the geometry described in Figure 2. A summary of the buckling and failure loads for all compression-loaded panels with a hole is shown in Figure 8, in which the filled bars represent the predicted buckling load, the crosshatched bars represent the experimentally determined first buckling load and the open bars represent failure. Three panel configurations are shown in the figure; type 1 with a 1.5-inch diameter hole in the weaker region for tailored panels, type 2 with a 3-inch

diameter hole in the weaker region for tailored panels and type 3 with a 3-inch diameter hole in the stiffer region of tailored panels. Only types 1 and 2 are shown for the straight-fiber panels since there are no stiffer regions. Each panel displayed significant post-buckling behavior. For all cases where the hole was in the weaker region of the panel, the overlap panel carried significantly higher buckling loads and failure loads than the corresponding tow-drop panel. Since the initial stacking sequence selection did not consider the possibility of the presence of holes in the stiffened region, the panels with the holes in the stiffened region did not demonstrate improved capability compared to straight-fiber panels.

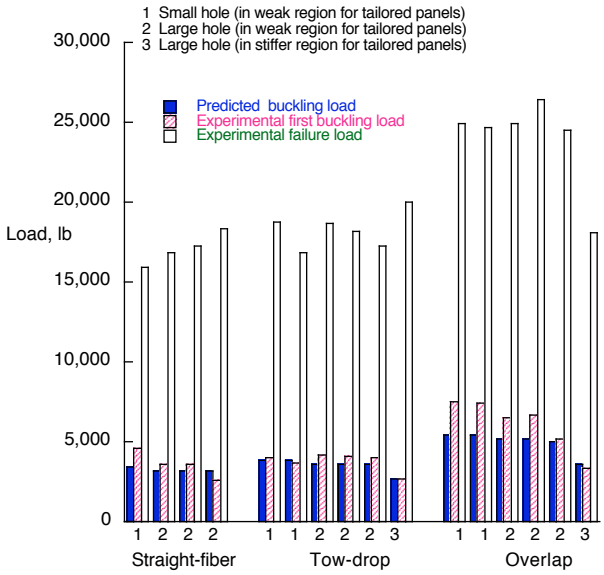

Figure 8. Compression-loaded panel buckling and failure loads.

Focus on overlap panels C5 and C6 to consider the mechanisms behind the relative magnitude of the initial buckling modes. These panels have similar tow-steered layups, however the central hole in panel C6 is in the stiffer region and the central hole in panel C5 is in the softer region. Earlier results postulated that the configuration of the panel C5 should increase the buckling load by steering the loads toward the restrained edges and reducing the stresses near the hole. Later design study results indicated that an increase in bending stiffness in the center may also contribute toward increased buckling values, if the presence of the hole did not produce undue degradation. To verify these claims, the in-plane stress resultant in the axial direction (calculated via STAGS) is displayed as a contour plot for panels C5 and C6 at a the pre-buckling load level of 500 lb in Figure 9a and b, respectively. In these plots the cooler colors represent higher compressive loads and the patterns of the stress fields follow the expected trends. However, the configuration of the panel C6 stiffness along with the presence of the hole leads to comparatively large stresses in the center of the panel (for a constant stiffness panel, the average value of the in-plane stress resultant for this load level would be around 33 lbs/in). Therefore even though the thicker middle section has an increased bending stiffness, the higher stress levels that are present due to the stiffness variation and the large hole dominate the buckling response and produce much lower buckling values than the corresponding C5 case. The same arguments hold true for the tow-drop case (B5 and B6). Smaller hole sizes along with stiffness variations designed specifically for this new mechanism may offer more improvement than demonstrated here.

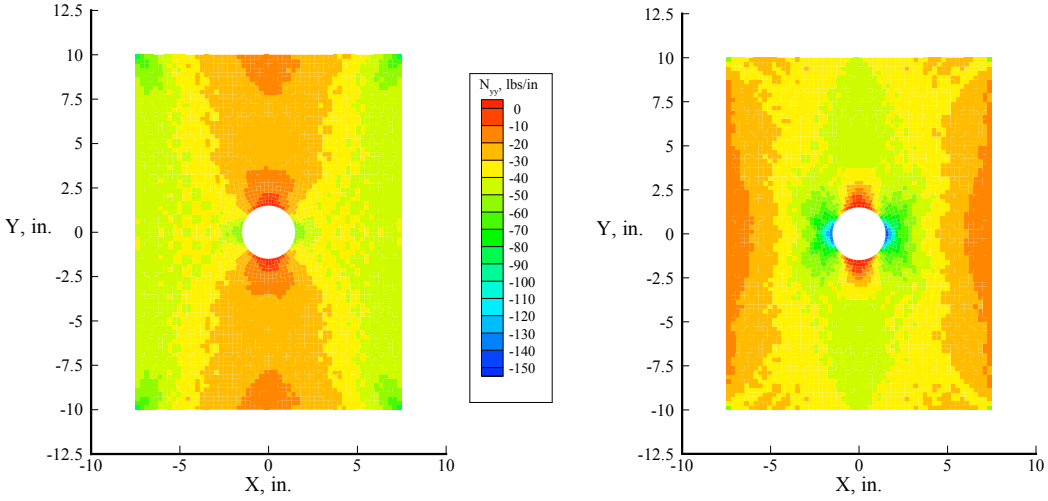

a) Panel C5 b) Panel C6

Figure 9. Axial in-plane stress resultant for overlap panels as determined by STAGS analysis at a load level of 500 lb.

Analytical and experimental displacement results for the compression loaded specimens are presented in Figure 10-Figure 12. End-shortening is represented by the red lines and out-of-plane deformations are represented by blue and green lines. Out-of-plane displacement measurement locations are shown in Figure 4. In each case, the solid line represents the experimental result and the dashed line represents the finite-element prediction. Results for the straight-fiber panel (A5) are shown in Figure 10. Similar results for the tow-drop panel with the hole in the un-stiffened region (B5) and the overlap panel with the hole in the un-stiffened region (C5) are shown in Figure 11 and Figure 12, respectively. These plots are similar to the test results from the earlier round of experiments and exhibit the same comparative magnitudes between the straight fiber, tow-drop, and overlap methods. Each panel buckles, carries additional load and then changes buckle pattern. Correlation between experimental displacement measurements and finite element predictions is excellent for the straight fiber and tow-drop cases far into the post-buckling realm, while the overlap panel C5 exhibits the general trends but with noticeably different load levels for buckling and mode switching.

Closer examination of the disparity between the experimental and analytical buckling loads is carried out through the use of the 3D visualization technique described earlier. Initially, strain data generated using this 3D visualization technique was compared directly to the strain gage readings from the actual test (for the strain gages indicated in Figure 4). Excellent agreement was demonstrated, so that full-field displacement and strain data from the 3D visualization system could be used in place of the smaller set of data locations that the strain gages offered. Contour plots of the axial surface strain as calculated by STAGS and from the actual test for a load of approximately 19,500 lb, which is well into the post-buckling range, are shown in Figure 13. The excellent agreement between the two plots verifies the ability of STAGS to correctly capture the response of these variable stiffness laminates. Furthermore, the capability of STAGS to predict the nonlinear response and mode switching, as demonstrated by the comparisons of the mode shapes in Figure 14 and Figure 15, provides the analyst and designer useful tools for subsequent investigation into tow-steered laminates.

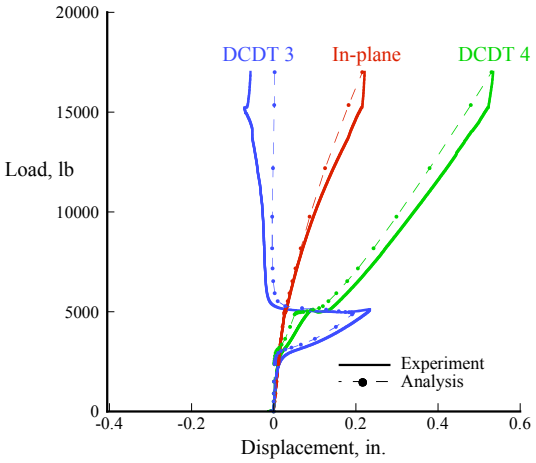

Figure 10. Load-displacement for panel A5.

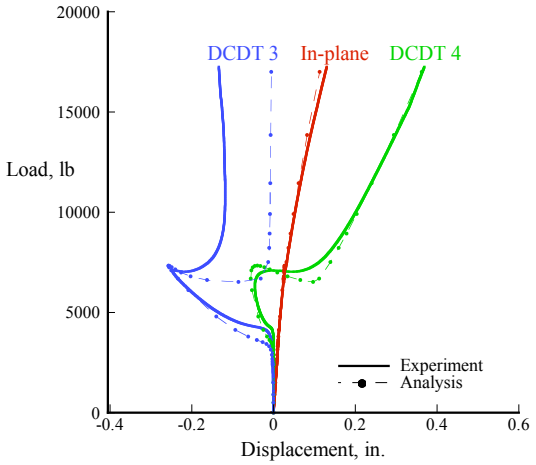

Figure 11. Load-displacement for panel B5.

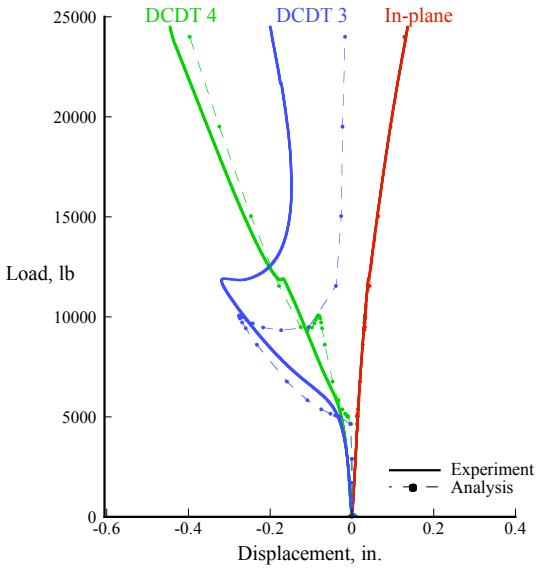

Figure 12. Load-displacement for panel C5.

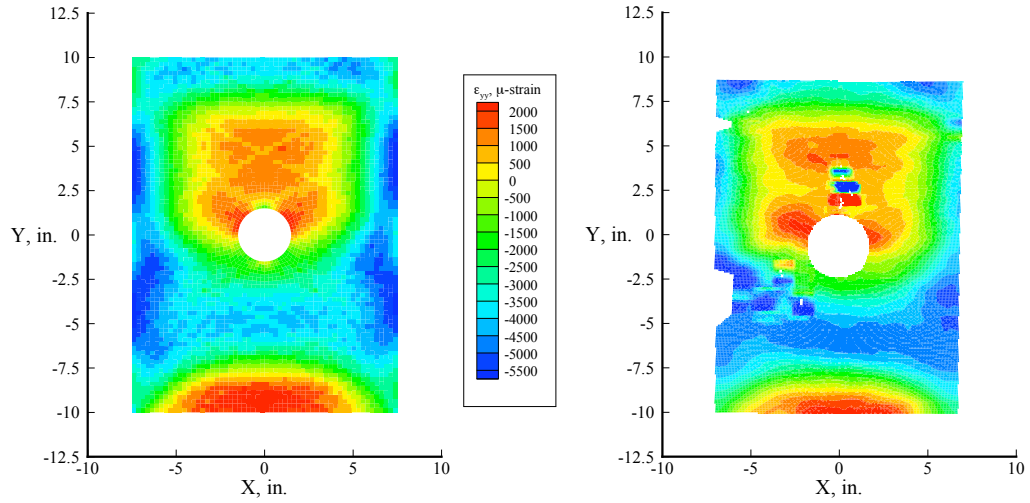

a) STAGS analysis: 19512 lb b) Experiment: 19629 lb

Figure 13. Axial surface strain component for compression panel C5.

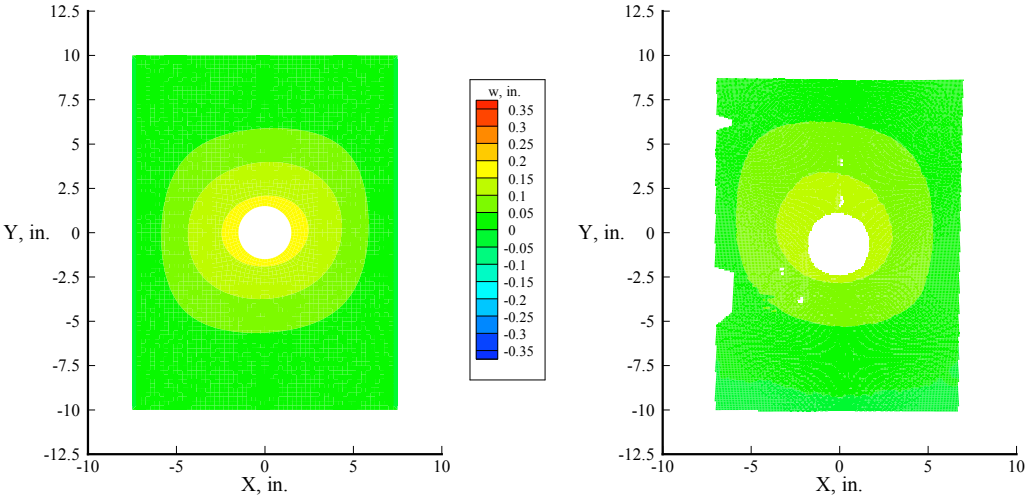

a) STAGS analysis: 6761.5 lb b) Experiment: 6797 lb

Figure 14. First mode shape of compression panel C5.

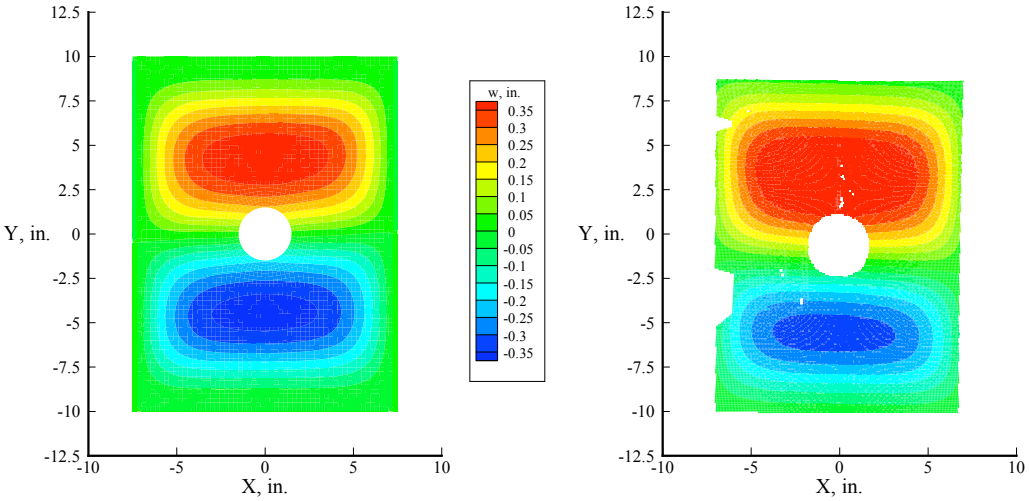

a) STAGS analysis: 19512 lb b) Experiment: 19629 lb

Figure 15. Second mode shape of compression panel C5.

Comparable results for the two panels with the hole located in the stiffer section of the tow-steered panel (B6 and C6) are presented in Figure 16 and Figure 17. The only significant discrepancy occurs for the panel C6, which undergoes a mode switch that was not captured by the nonlinear STAGS analysis. The first mode shape for this panel is similar to the one shown in Figure 14 for panel C5, which represents a buckled mode shape of one half-wave in each direction. Plots of the predicted and actual mode shapes for panel C6 near a load of 12,500 lb are shown in Figure 18. Note that the second mode shape from the experiment is the same mode shape as the first except for a different out-of-plane direction. This phenomenon was not predicted by STAGS due to the straight-forward manner in which initial imperfections are introduced within the program. Consideration of actual measured imperfections of the panel may produce more accurate results.

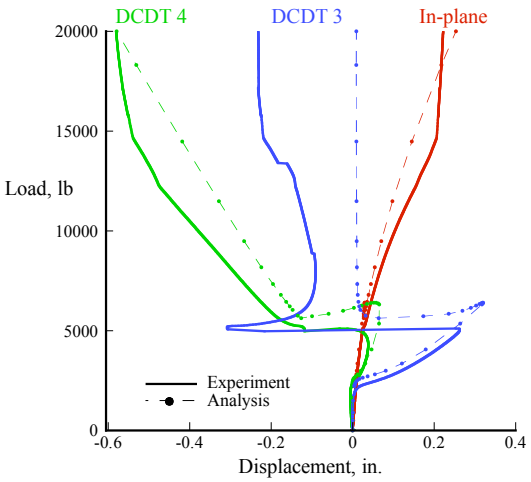

Figure 16: Load-displacement for panel B6

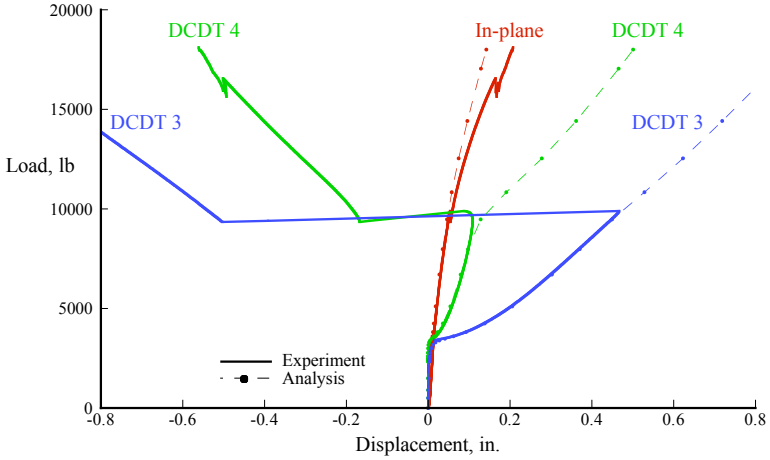

Figure 17. Load-displacement for panel C6.

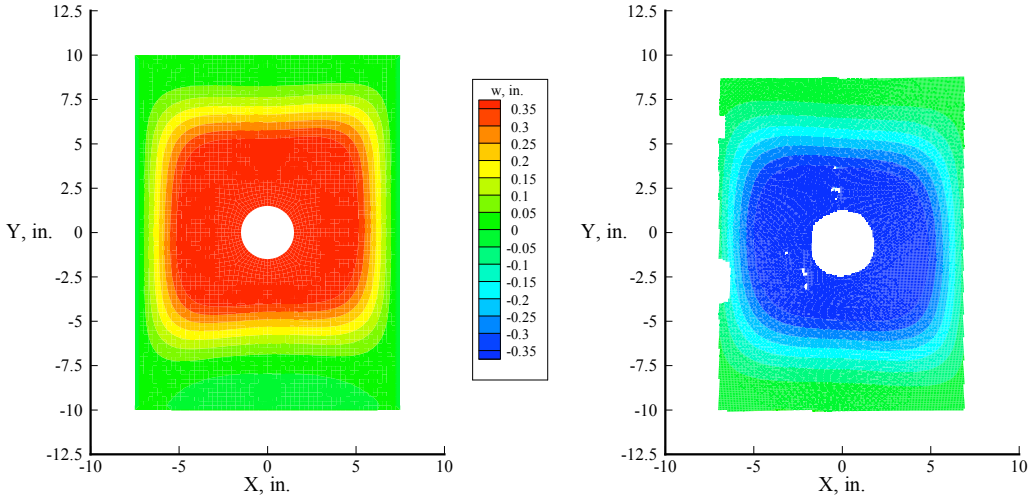

a) STAGS analysis: 12535 lb b) Experiment: 12496 lb

Figure 18. Second mode shape of compression panel C6.

B. Shear Loaded Panels

The tow-steered panels were not optimized for shear loading, however, the ability to carry shear load and accurately predict behavior due to shear loading is critical to their successful application to aircraft structures. One shear-loaded panel was cut from each sheet, producing a total of three panels representative of the three construction techniques. Each shear panel was loaded by applying a tensile load along one diagonal with the picture-frame fixture holding the edges straight and enforcing a defined set of boundary conditions. The initial buckling load predicted by finite element analysis and determined experimentally, as well as the failure load, are shown in Figure 19, in which the filled bars represent the predicted buckling load, the crosshatched bars represent the experimentally determined buckling load and the open bars represent failure. Buckling loads determined through analysis and experiment are in good agreement for the tow-steered panels. Each panel sustained loads significantly greater than the buckling load. While the buckling loads are not significantly greater for the tow-steered panels than for the straight fiber panel, the evaluation of the shear panels indicates that the bucking behavior is accurately predicted, indicating that optimization for shear loading might be used to design panels with significant weight savings compared to traditional straight-fiber panels.

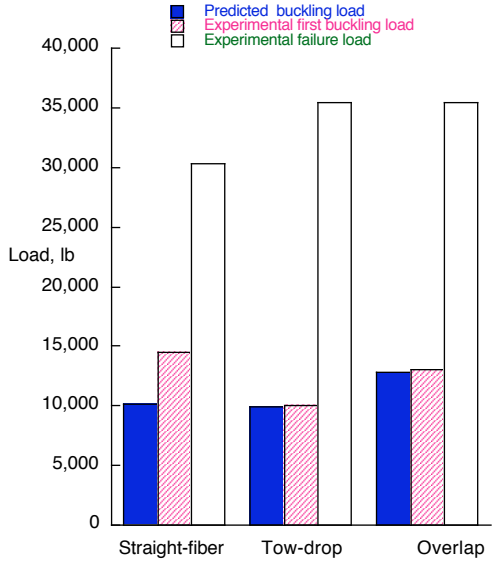

Figure 19. Shear-loaded panel buckling and failure loads.

Analytical and experimental out-of-plane displacement results for the shear-loaded specimens with central holes are presented in Figure 20-Figure 22. The solid lines represent the experimental results and the dashed lines represent the finite-element predictions, where the measurement locations are shown in Figure 5. Results for the straight-fiber panel (A7) are shown in Figure 20. Similar results for the tow-drop panel (B7) and the overlap panel (C7) are shown in Figure 21 and Figure 22, respectively. Good agreement can be seen for prebuckling and the initial post-buckling behavior in each case, though the prediction is less accurate as the loading is increased. The out-of-plane deformation patterns for panel C7 for a load of approximately 15,000 lb are shown in Figure 23. The out-of-plane displacements shown agree in their general trends, but the analysis predicted increased displacement than the experiment displayed. In addition, the experimental results indicate that the regions near the corners away from the loaded diagonal are moving in the opposite direction as the region near the hole. This behavior is not captured well by the analysis at this load level.

Contour plots of the surface strain along the loading diagonal as calculated by STAGS and from the experiment of panel C7 are shown in Figure 24. The strains for a load of approximately 10,000 lb are shown in Figure 24a and

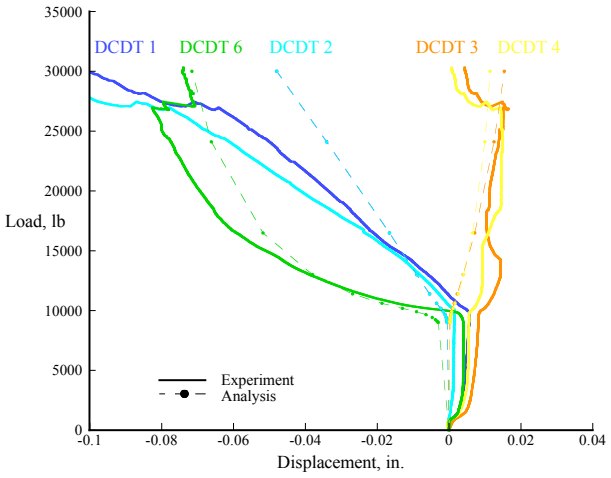

Figure 20. Load-displacement for shear panel A7.

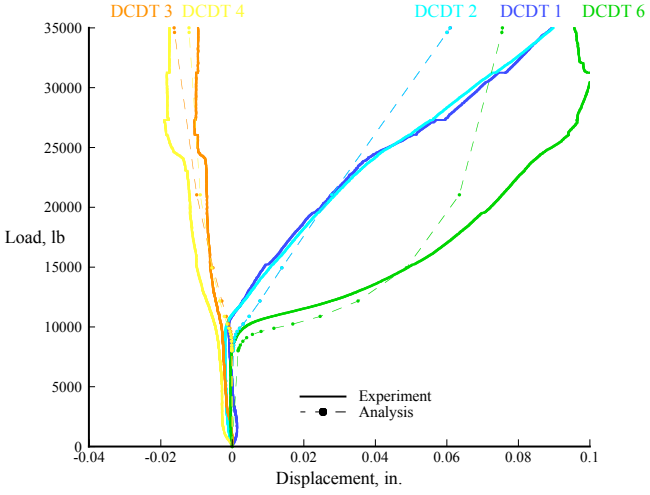

Figure 21. Load-displacement for shear panel B7.

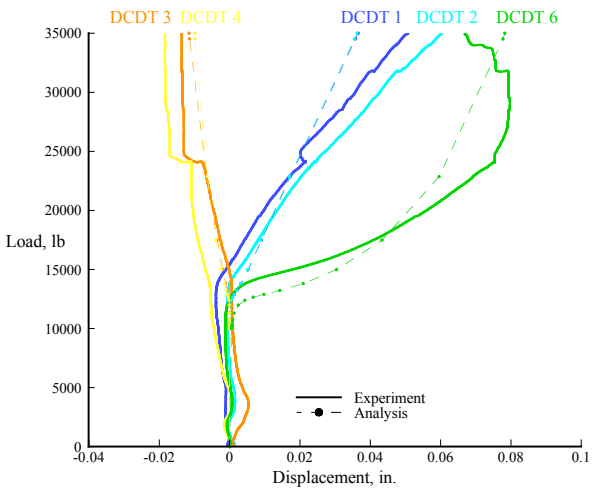

Figure 22. Load-displacement for shear panel C7.

b, while strains for a load of approximately 15,000 lb are shown in Figure 24c and d. Analytical and experimental results for the shear-loaded panels agree somewhat in the lower load ranges and but do not agree as well as the compression-loaded panels. A comparison of strain behavior demonstrates a difference in that the experiment shows significantly lower values of strain along the loading diagonal than in the analysis. Strain concentrations around the hole edge are not as large in the experiment as in the analytical predictions. This discrepancy may be due to the more complicated load introduction of the fixture, which may not have been adequately modeled, and the influence of assumed, rather than measured, initial imperfections in the analysis. More refinement of the analytical technique is needed to adequately capture the behavior of the shear-loaded panels.

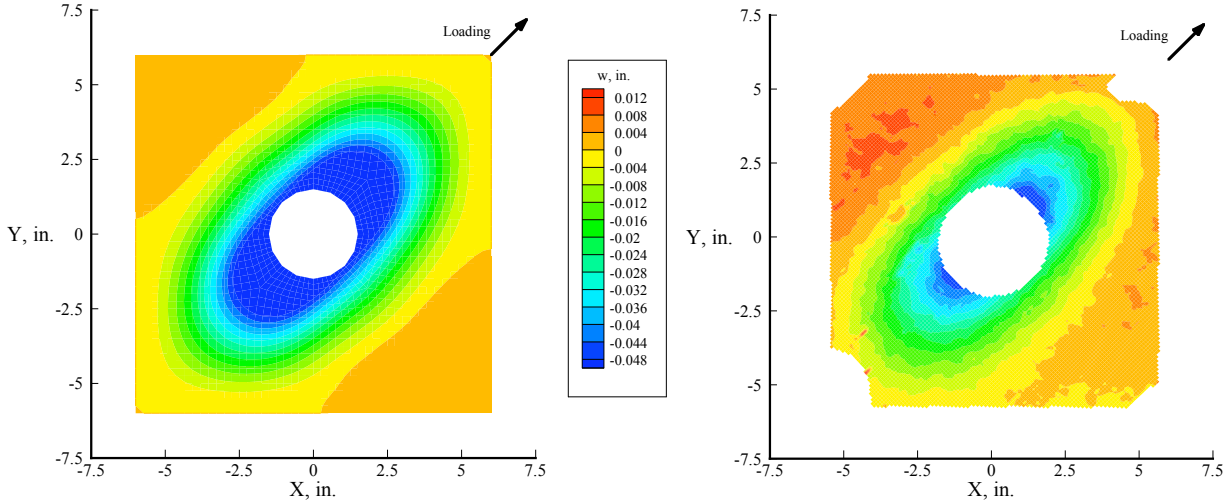

a) STAGS analysis: 14988 lb

b) Experiment: 14971 lb

Figure 23. First Mode Shape of Shear Panel C7.

V. Concluding Remarks

Compression- and shear-loaded graphite epoxy flat panels were evaluated in this study to determine their buckling and post buckling behavior. Experimental verification of the response and buckling characteristics of these tow-steered panels represents a major step toward implementation of this elastic tailoring concept in the aeronautic industry. The ability to model the complex stiffness variation of optimized tow-steered panels through finite element analysis allows the designer to assess the effect of curvilinear tow paths in an initial design study. Furthermore, the fact that the novel construction techniques, using tow-drop and overlap plies, did not produce any unforeseen failure mechanisms establishes tow-steering as a viable design concept. This study has verified the potential of fabricating variable stiffness tow-steered specimens designed to meet specified load conditions which could be applicable to aircraft structures.

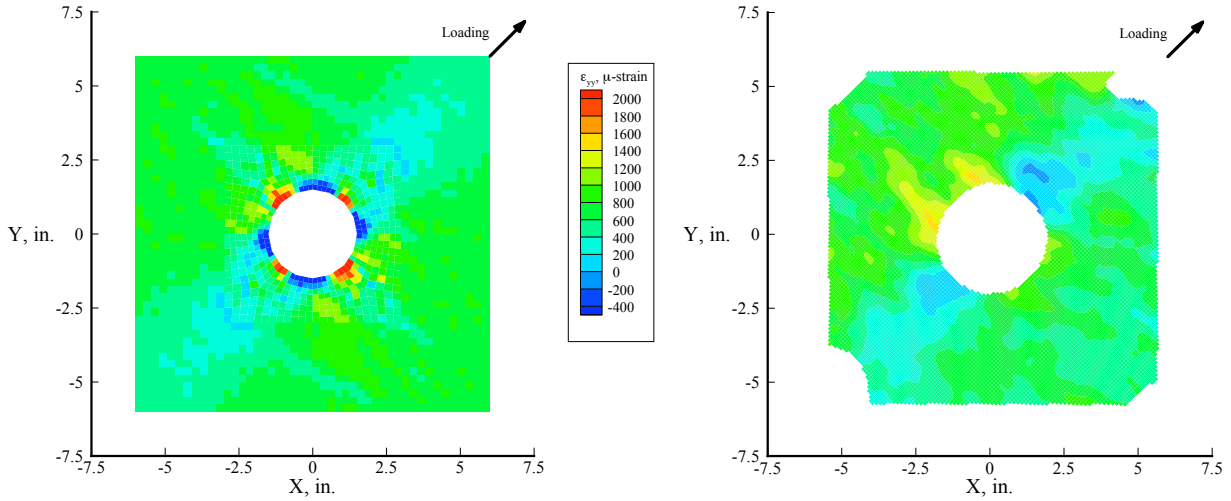

a) STAGS analysis: 10050 lb

b) Experiment: 10020 lb

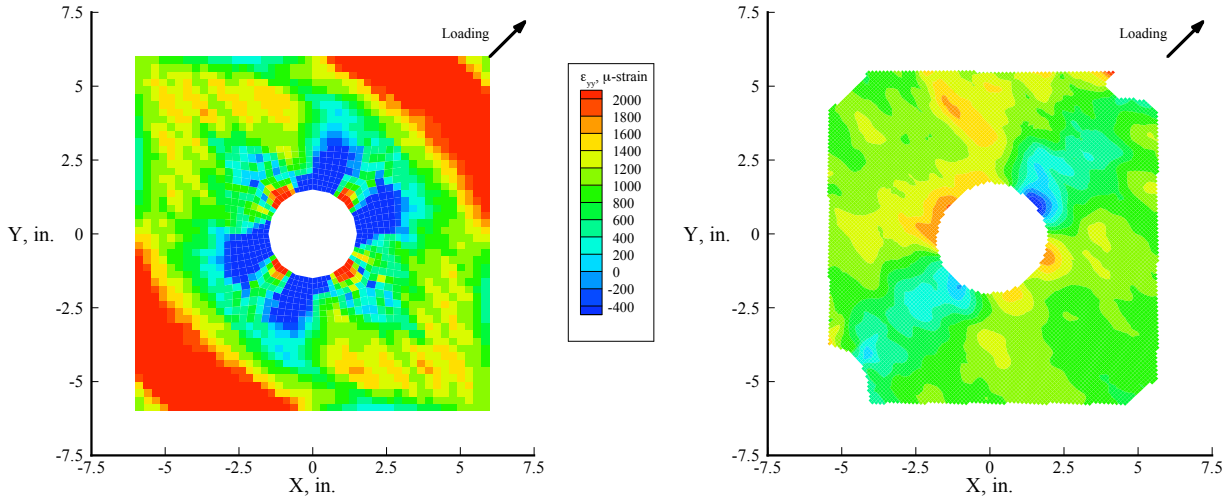

a) STAGS analysis: 14988 lb

b) Experiment: 14971 lb

Figure 24: Diagonal surface strain component for shear panel C7

References

1. Gürdal, Z., Haftka, R.T., and Hajela, P., Design and Optimization of Laminated Composite Materials, John Wiley and Sons, Inc., New York, NY, 1999, pp. 185-218.

2. Hyer, M. W., and Charette, R. F., "The Use of Curvilinear Fiber Format in Composite Structure Design," Proceedings of the 30th AIAA/ASME/ASCE/AHS/ASC Structures, Structural Dynamics and Materials (SDM) Conference, New York, NY, 1989, paper no 1404.

3. Nagendra, S., Kodiyalam, A., Davis, J. E., and Parthasarathy, V. N., "Optimization of Tow Fiber Paths for Composite Design," Proceedings of the 36th AIAA/ASME/ASCE/AHS/ASC Structures, Structural Dynamics and Materials (SDM) Conference, New Orleans, LA, April 1995. AIAA paper no. 1275.

4. Gürdal, Z., and Olmedo, R., "In-Plane Response of Laminates with Spatially Varying Fiber Orientations: Variable Stiffness Concept," AIAA Journal, Vol. 31, (4), April 1993, pp. 751-758.

5. Hyer, M. W., and Lee, H. H., "The Use of Curvilinear Fiber Format to Improve Buckling Resistance of Composite Plates with Central Holes," Composite Structures, Vol. 18, 1991, pp. 239-261.

6. Olmedo, R., and Gürdal, Z., "Buckling Response of Laminates with Spatially Varying Fiber Orientations," Proceedings of the 34th AIAA/ASME/ASCE/AHS/ASC Structures, Structural Dynamics and Materials (SDM) Conference, La Jolla, CA, April 1993, paper no. 1567.

7. Waldhart, C. J., Gürdal, Z., and Ribbens, C., "Analysis of Tow Placed, Parallel Fiber, Variable Stiffness Laminates," Proceedings of the 37th AIAA/ASME/ASCE/AHS/ASC Structures, Structural Dynamics and Materials (SDM) Conference, Salt Lake City, UT, April 1996, paper no. 1569.

8. Evans, D. O., Vaniglia, M. M., and Hopkins, P. C., "Fiber Placement Process Study," 34th International SAMPE Symposium, May 1989.

9. Tatting, B. F., and Gürdal, Z., "Design and Manufacture of Tow-Placed Variable Stiffness Composite Laminates with Manufacturing Considerations," Proceedings of the 13th U.S. National Congress of Applied Mechanics (USNCAM), Gainesville, FL, 1998.

10. Wu, K. C., and Gürdal, Z., "Thermal Testing of Tow-Placed Variable Stiffness Panels," Proceedings of the 42nd AIAA/ASME/ASCE/AHS/ASC Structures, Structural Dynamics and Materials (SDM) Conference, Seattle, WA, April 2001, paper no 1190.

11. Wu, K. C., Gürdal, Z., and Starnes, J. H., "Structural Response of Compression-Loaded, Tow-Placed, Variable Stiffness Panels," Proceedings of the 43rd AIAA/ASME/ASCE/AHS/ASC Structures, Structural Dynamics and Materials (SDM) Conference, Denver, CO, April 22-25, 2002. Available as AIAA 2002-1512.

12. Gürdal, Z., Tatting, B. F. and Wu, K. C., "Tow-Placement Technology and Fabrication Issues for Laminates Composite Structures," Proceedings of the 46th AIAA/ASME/ASCE/AHS/ASC Structures, Structural Dynamics and Materials (SDM) Conference, Austin TX, April 2005.

13. Jegley, D., Tatting, B. F. and Gürdal, Z., "Optimization of Elastically Tailored Tow Placed Plates with Holes," Proceedings of the 44th AIAA/ASME/ASCE/AHS/ASC Structures, Structural Dynamics and Materials (SDM) Conference, Norfolk VA, April 2003, AIAA Paper No. 1420.

14. Tatting, B. F., and Gürdal, Z., Automated Finite Element Analysis of Elastically-Tailored Plates, NASA CR 2003-212679, December 2003.

15. Tatting, B. F., and Gürdal, Z., Design and Manufacturing of Elastically Tailored Tow Placed Plates, NASA CR 2002-211919, August 2002.

16. Rankin, C. C., Brogan, F. A., Loden, W. A., and Cabiness, H. D., "STAGS Users Manual," Lockheed Martin Missiles & Space Co., Inc., Report LMSC P032594, June 2000.

17. Rouse, M., "Postbuckling and Failure Characteristics of Stiffened Graphite-Epoxy Shear Webs," Proceedings of the 28th AIAA/ASME/ASCE/AHS/ASC Structures, Structural Dynamics and Materials (SDM) Conference, Monterey CA, April 1987, AIAA Paper No. 733.

18. Helm, J. D., McNeil, S. R., and Sutton, M. A., "Improved Three-Dimensional Image Correlation for Surface Displacement Measurements," Optical Engineering, Vol. 35, No. 7, July 1996, pp. 1911-1920.